ELSEVIER

International Journal of Mass Spectrometry 204 (2001) 223–232

International Journal of Mass Spectrometry

Photodissociation of exohedral transition metal–C_{60} complexes

G.A. Grieves, J.W. Buchanan, J.E. Reddic, M.A. Duncan*

Department of Chemistry, University of Georgia, Athens, Georgia 30602, USA

Abstract

Laser ablation/vaporization of solid metal samples coated with thin films of C_{60} is employed in a pulsed-nozzle cluster source to produce various transition metal–C_{60} complexes. Mass spectra contain species of the form $M_x(C_{60})_y$, where $x = 1–5$ and $y = 1,2$. Mass-selected photodissociation studies investigate the structural and bonding properties of these complexes. Photodissociation shows primarily the elimination of metal in all complexes, demonstrating that the complexes are exohedral. Atomic and molecular desorption of metal are observed in different situations, suggesting that these complexes have metal dispersed to some degree as "films" on the fullerene surface. Some clusters fragment by loss of metal carbides (e.g. $C_{59}Fe^+$, $V_3C_4^+$), indicating insertion of metal into the fullerene cage wall. (Int J Mass Spectrom 204 (2001) 223–232) © 2001 Elsevier Science B.V.

Keywords: Clusters; Metallo-fullerenes; Photodissociation

1. Introduction

Since the discovery of C_{60} and the fullerenes, there has been much interest in doping fullerene clusters with metal [1]. Endohedral metallo-fullerenes, which have one or more metal atoms inside the fullerene cage, have been studied for both main group and transition metals [1–6]. There has been significant recent progress in the isolation of these materials in useful quantities [1–6]. Alkali metal–C_{60} solids have been synthesized which exhibit superconductivity [7,8]. In related work, metals are used to catalyze carbon nanotube formation [1] and some metal-filled nanotubes have been produced [9,10]. Gas phase studies have shown that many metal ion–C_{60} complexes can be produced and studied in mass spectrometers, although there are few measurements of specific properties for these species [11–16]. Martin and co-workers have shown that multiatom metal layers can be produced on the surface of C_{60} or C_{70} molecules [17–21]. They have demonstrated layer formation for several metals and have seen magic numbers attributed to geometric packing of atoms on the fullerene surface. Our group [22] and that of Kaya and co-workers [23–28] have also reported different methods for the production of multiple metal atoms attached to the exterior surface of C_{60}. Kaya and co-workers observed the formation of multimetal/multi–C_{60} networks and suggest fascinating structural patterns [23–28]. There is therefore an emerging area of interest in the properties of such exohedral metallofullerenes. In certain complexes produced under "exohedral" conditions, fragmentation [19–21] and/or ion mobility measurements [29,30] indicate metal incorporation into the fullerene cage wall. In the present article, we use mass-selected laser photodissociation

* Corresponding author. E-mail: maduncan@arches.uga.edu.

PII S1387-3806(00)00362-6

to further investigate the structures and bonding configurations in these kinds of metal–C_{60} complexes.

Martin and co-workers have produced multitransition metal atom coatings of individual fullerene molecules by way of a combined inert gas condensation source employing laser vaporization of metal and a fullerene oven. They detected clusters with ArF (193 nm) multiphoton ionization. Studies as a function of laser power revealed some fragmentation processes which included the elimination of metal and the surprising formation of metal carbide clusters. With titanium and vanadium, the familiar M_8C_{12} "metcars" clusters [31] were produced, whereas niobium and tantalum produced various "nanocrystal" metal carbide clusters which were inferred from the near 1:1 M:C stoichiometries. In more recent studies, by our group [22] and that of Martin and co-workers [19–21], the clusters were mass-selected for photodissociation studies. In silver–C_{60} complexes [22], the weak metal–fullerene interaction led to elimination of molecular metal units (e.g., Ag_3^+). In niobium and tantalum, a surprising channel of sequential C_3 loss was observed [19–21]. Since fullerenes are well known to eliminate C_2 in photodissociation, the suggestion arose that these clusters might not be fullerenes. However, Fye and Jarrold performed ion mobility measurements on these same niobium–C_{60} masses and concluded that their structures are fullerenelike [29]. This led to the suggestion that Nb_x–C_{60} masses might represent clusters with one or more metal included in the fullerene cage wall, which thus modified the photofragmentation processes. This had been suggested for the $x = 1$ species in earlier work by Jarrold and co-workers [30]. These results and others suggest that metal–C_{60} aggregates may exhibit novel structural patterns and unusual photodissociation dynamics.

In the present article, we extend these photodissociation methods to investigate other small M–C_{60} clusters and M_x–$(C_{60})_2$ clusters for M = V, Fe, Co, Ni, and Ti. In every case masses are observed of the form M_x–$(C_{60})_y$, with x varying from 1 to 5 and y = 1,2. Mass selected photodissociation of these complexes results in several interesting decomposition pathways. We see simple elimination of metal from the fullerene surface as both atomic and molecular species. In some clusters, the formation of metal carbide fragments is competitive with metal loss. These fascinating processes vary with the metal under consideration, with the number of metal atoms present, and even with the conditions of preparation of the clusters.

2. Experimental

Transition metal–C_{60} complexes are produced in a laser vaporization cluster source with specially prepared sample rods. A 1/4 or 1/2 in. diameter rod of the desired metal is coated with a sublimed film of C_{60} on its surface. C_{60} films are prepared in a vacuum chamber separate from the molecular beam apparatus. A sublimation oven is constructed from a one-fourth in. diameter ceramic tube wrapped with a nichrome wire heater. The oven is loaded with C_{60} powder (MER Corporation) and heated with a variac until visible sublimation occurs on the vacuum chamber windows. The sample rod is mounted on a rotating stage about two inches from the oven. No effort is made to quantify the film thickness, but variac settings are used to achieve reproducible films.

The metal rod sample coated with C_{60} is transferred immediately to the molecular beam machine and mounted in a rotating rod cluster source. This source is of standard design, but uses a modified Newport nozzle [32]. Vaporization is accomplished with the second harmonic or third harmonic of a Nd:YAG laser (532 or 355 nm). We use laser powers somewhat lower than those typically employed for pure metal vaporization (about 10–20 mJ/pulse). If the laser power is too low, we observe C_{60} in the molecular beam without attached metal. At higher powers, we observe primarily metal atoms. Intermediate settings make it possible to vaporize the C_{60} from the film without dissociating it and to vaporize the underlying metal at the same time. Expansion of this mixture produces the desired metal–C_{60} complexes. Cation clusters are extracted from the molecular beam into the mass spectrometer with pulsed acceleration voltages. The beam apparatus and mass

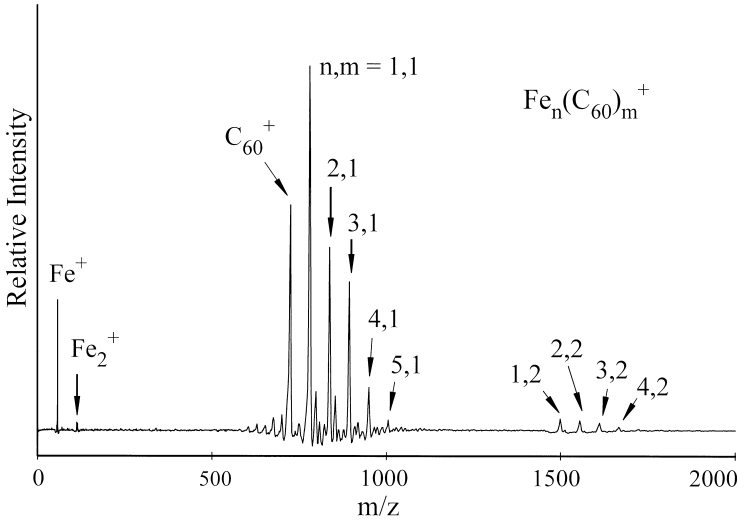

Fig. 1. Mass distribution of cation clusters produced with laser ablation/vaporization of an iron rod coated with a film of C_{60}.

spectrometer for these experiments have been described previously [33]. Photodissociation of mass-selected clusters is accomplished with either the second or third harmonic of a Nd:YAG laser (532 or 355 nm). Laser power dependences are used to investigate the role of multiphoton processes.

3. Results and discussion

Fig. 1 shows a representative mass spectrum obtained when a film-coated iron rod is treated with laser ablation/vaporization and the resulting cation clusters are measured with the time-of-flight mass spectrometer. As shown, there are prominent mass peaks corresponding to various numbers of iron atoms attached to C_{60} and much smaller intensity peaks corresponding to metals clustered with two C_{60} molecules. Mass spectra similar to this are measured for a variety of transition metals including Ni, Co, V, etc. There is only a minor amount of fragmentation of the fullerene. Apparently, C_{60} is stable enough to survive the plasma conditions and therefore the metal in these complexes is expected to be attached to its exterior surface. Fragmentation experiments described below address this issue more directly.

The total number of metals added to C_{60} by this ablation method is much less than in the clusters studied by Martin and coworkers, where 20–40 transition metals were routinely incorporated into the clusters [17–21]. Likewise, the double-rod source of Kaya and co-workers provides more C_{60} concentration, and more multi-C_{60} clusters are formed [23–28]. This is due in part to the source conditions we have chosen, which do not produce pure metal clusters in any significant concentrations. The mass spectrum shows that the only pure metal clusters seen under these conditions are dimers, whereas adducts containing up to five metal atoms are seen in the complexes with one and two C_{60} molecules. This suggests that the clusters here grow by successive addition of metal atoms (or perhaps dimers) to C_{60} rather than by the addition of larger metal clusters to C_{60}. It is therefore conceivable that metal attaches to C_{60} as an “island” on the surface, where additional atoms bind to earlier ones, or that metal exists on the surface more like a “film” where individual atoms bind to specific surface sites on the fullerene. Important considerations in these processes would be the relative bond energies within pure metal clusters compared to the metal–C_{60} bond energies. Bonding energetics are known for many small transition metal clusters (see Table 1) [34], but bond energies are not known for metal–C_{60}

Table 1
Energetic parameters for small iron and vanadium clusters relevant for this work, all units are electron volts

Cluster	IP	D_0 (neutral)[a]	D_0 (cation)[a]
V	6.74	. . .	. . .
V_2	6.10,[b] 6.357[c]	2.75	3.14
V_3	5.49,[b] 5.498[d]	1.42	2.27
V_4	5.63,[b] 5.659[d]	3.67	3.53
Fe	7.87	. . .	. . .
Fe_2	6.30[e]	1.14	2.74
Fe_3	6.4–6.5[e]	1.82	1.67
Fe_4	6.4–6.5[e]	2.06	2.11

[a] See [34].
[b] See [36].
[c] See [37].
[d] See [38].
[e] See [39].

interactions. However, it is not clear how aggregation of metal may influence the metal–C_{60} bond energetics or how adsorption on the fullerene surface may moderate the metal–metal bonding.

Figs. 2–7 show photodissociation experiments of mass selected metal–C_{60} complexes. In these experiments, the data are accumulated with a computer difference method with the photodissociation laser "on" versus "off." The negative going mass peak reflects the dissociation of the mass-selected parent ion while the positive signals indicate the photofragments coming from this parent. If all parent and fragment ions were collected with equal efficiency, charge conservation would cause the integrated area of fragment peaks to sum to the area of the parent ion depletion. However, the focusing of our instrument does not allow this and we usually adjust the conditions to optimize the fragment intensities. The data shown here are all accumulated at 355 nm. In data not shown, we have measured essentially the same fragmentation patterns at 532 nm. In all spectra, we adjust the laser power to minimize multiphoton processes. However, power dependences are usually nonlinear, indicating that multiple photon absorption is necessary to cause fragmentation of these clusters on the 2–3 μsecond time scale of residence in our interaction region.

Fig. 2 shows the data for mono-metal–C_{60} com-

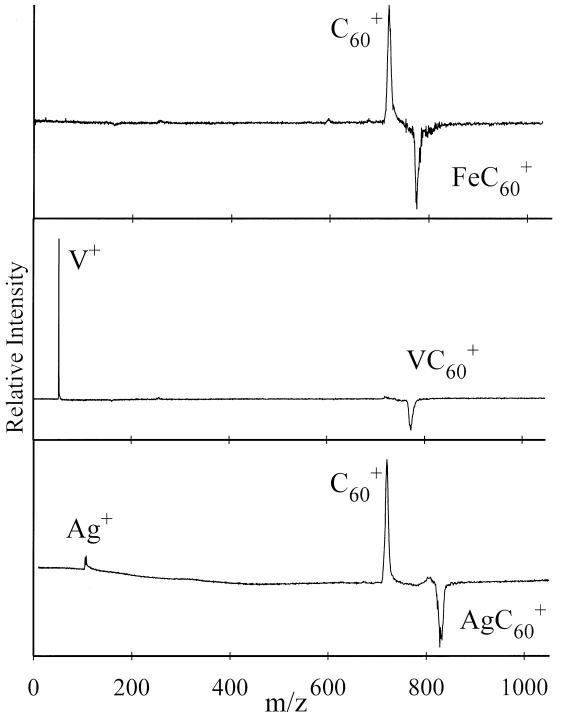

Fig. 2. Photodissociation of mono-metal complexes with C_{60}. The prominent fragments can be predicted based on ionization potentials of the metal compared to that of C_{60}.

plexes of iron, vanadium and silver. These data illustrate the importance of the relative ionization potentials of the metal and C_{60} in these fragmentation processes. In the case of Fe–C_{60}^+, iron has a higher ionization potential (IP = 7.87 eV) than C_{60} (IP = 7.58 eV [1]). The lowest energy fragmentation process therefore leaves the charge on the lower IP fragment C_{60} and iron is eliminated as neutral atoms. The reverse is true in the case of vanadium (IP = 6.74 eV), and charged atoms are eliminated leaving behind neutral C_{60}. In the case of silver, the IP (7.576 eV) is very close to that of C_{60} and not surprisingly both fragmentation channels are observed. In all of these complexes, the expected lowest energy channels are measured, and there is no evidence for fragmentation of the fullerene moiety. It is therefore clear that these mono-metal complexes represent exohedral metal adsorption on the fullerene surface. In the case of Fe–C_{60}^+, we have previously described competitive binding experiments with benzene and coronene li-

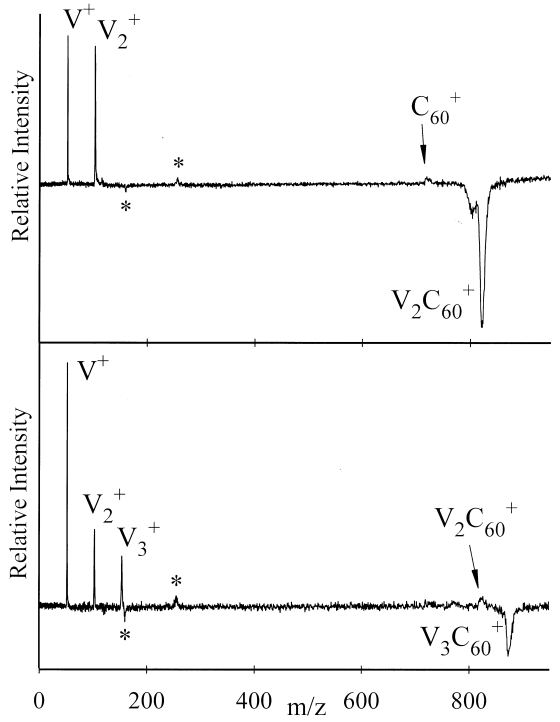

Fig. 3. Photodissociation at 355 nm of vanadium–C_{60} complexes with two and three metal atoms under so-called cold conditions. Metal atoms, dimers, and trimers are all seen as prominent fragments. The asterisks mark known artifact peaks from electrical noise in the system, which is independent of the excitation laser.

gands which bracketed the Fe binding energy as less than 49 kcal/mol [35].

Fig. 3 shows the photodissociation at 355 nm of vanadium–C_{60} complexes with two and three metal atoms. The products observed are the respective metal atom, dimer and trimer, with the metal atom by far the most abundant in the V_3–C_{60}^+ system. A small amount of C_{60}^+ fragment is also detected. These fragmentation channels are unchanged at 532 nm and the relative intensities of these peaks are invariant with the laser power. The metal fragments all have ionization potentials less than that of C_{60}, as indicated in Table 1, and therefore the desorption of charged metal fragments rather than C_{60}^+ is expected. As also shown in Table 1, V_2^+ and V_3^+ have substantial bonding stability, and it is therefore not surprising that these metal molecules would be desorbed intact if they existed on the surface. It is interesting to consider what photodissociation dynamics could produce these fragments. We assume that metal adsorbs as atoms, because as noted above there are no pure metal clusters present in the mass spectrum. It is possible that metal adsorbed on the C_{60} surface aggregates as islands with metal–metal interactions as well as metal–surface interactions. The desorption of metal dimers and trimers then indicates that these species were present on the surface. It also conceivable that the metal exists only as separated atoms on the surface, but then it is difficult to explain the molecular metal products. A mechanism of surface diffusion of atoms followed by aggregation prior to desorption seems unlikely. Atomic fragments might come from desorption of clusters/island on the surface which then fragmented in the process of desorption. However, desorption of a metal trimer, for example, followed by fragmentation down to atoms is a relatively high energy process, as can be seen from the metal cluster thermochemistry in Table 1. This sequential fragmentation process should vary with the laser power, and no such variation is observed. It seems more likely that atomic fragments come from direct desorption of adsorbed atoms. The most likely scenario then, is that these fragmentation channels represent approximately the distribution of species which are actually adsorbed. A distribution of adsorbed species present indicates that surface mobility of metal after adsorption is limited, i.e. that atoms bind to the surface or to growing islands of metal depending on the statistics of their landing. Once adsorbed, atomic and molecular metal species interact strongly with the fullerene surface. This is in sharp contrast with our previous results on silver–C_{60} complexes, in which completely intact molecular species were eliminated without any atomic fragments [22].

Fig. 4 shows another view of fragmentation of vanadium–C_{60} complexes, again with two and three atoms of metal and again with excitation at 355 nm. These spectra were measured on a different day from those shown in Fig. 3, but all other experimental parameters were intended to be the same. Clearly the outcome of these experiments was different. V_2–C_{60}^+ fragments here to primarily dimers and atoms, but now the ratio of dimers is much higher. Additionally,

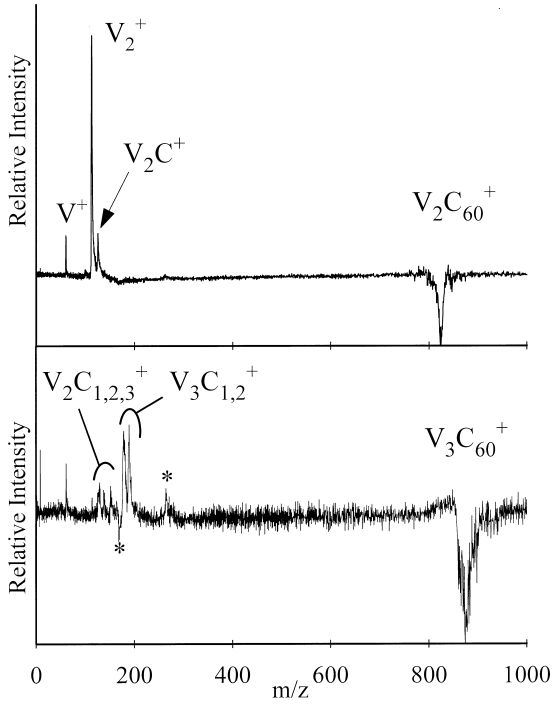

Fig. 4. Photodissociation at 355 nm of vanadium–C_{60} complexes with two and three metal atoms under so-called warm conditions. Metal atoms, dimers, and trimers are all seen as fragments, but significant amounts of metal–carbide fragments are also measured. The asterisks mark known artifact peaks from electrical noise in the system.

the new fragment ion V_2C^+ is observed. V_3–C_{60}^+ has fewer pure metal fragments, and there are now several metal carbide fragments (V_2C_x where $x = 1$–13 and V_3C_y where $y = 1,2$). It is surprising that the data in Figs. 3 and 4 are so different, when all experimental variables were intended to be the same and when the mass distribution out of the source appeared to be the same. The only difference we can suggest between these experiments is the temperature of the clusters during their growth. There is of course no way to measure the temperature of the clusters in these experiments, and so adjustments on the source are made to produce the largest amount of clustering. On different days the performance of the pulsed gas valve may vary slightly in amplitude or in timing, and the relationship between this and the vaporization laser has a nonlinear effect on the collisional rate and cooling of the clusters. We speculate therefore that these two experiments represent different cluster growth conditions, with the data in Figs. 3 and 4 representing "colder" and "warmer" conditions, respectively. It is reasonable that if the complexes are hot then surface mobility of atoms would be greater, and there might be a larger fraction of diatomic metal compared to atoms, as seen for V_2–C_{60}^+ in Fig. 4. The formation of metal carbide fragments indicates that the metal has reacted with the carbon cage wall and inserted into it. Again, it is reasonable that there would be an activation energy for insertion and that hotter growth conditions would promote this process. It is also interesting to note that the amount of insertion is much greater for V_3–C_{60}^+ than it is for V_2–C_{60}^+, Apparently, a cluster with more metal is better able to undergo insertion into the cage. A similar size effect on metal insertion into the cluster wall was seen previously for Martin and co-workers in the fragmentation of niobium– and tantalum–fullerene complexes [19–21].

The theme of metal insertion into the cage wall is demonstrated again in the case of V_4–C_{60}^+ which was studied under the so-called warmer growth conditions. In Fig. 5 the dissociation of this cluster is shown to produce some V^+, but the only molecular fragment is $V_3C_4^+$. The signal levels in this experiment are low reflecting the low efficiency (or slow rate) of dissociation in this system. However, this result is reproducible. This result and those in Fig. 4 are consistent with those of Martin on larger V_x–C_{60}^+ complexes, where a distribution of metal carbide fragments were obtained and the met-car $V_8C_{12}^+$ was a prominent fragment. Our results show that efficient insertion into the fullerene wall begins at a very small number of metal atoms and that this chemistry depends on the growth temperature. Another observation is that the photodissociation cross section is much smaller for these reacted clusters produced under "warm" conditions, as evidenced by the noisier data. Apparently the structure of the clusters is dramatically different due to their growth conditions. The laser conditions are the same in both experiments. Thus the insertion chemistry happened in the growth process and was not the result of any photochemistry from the laser excitation.

Fig. 6 shows similar measurements for iron–C_{60}

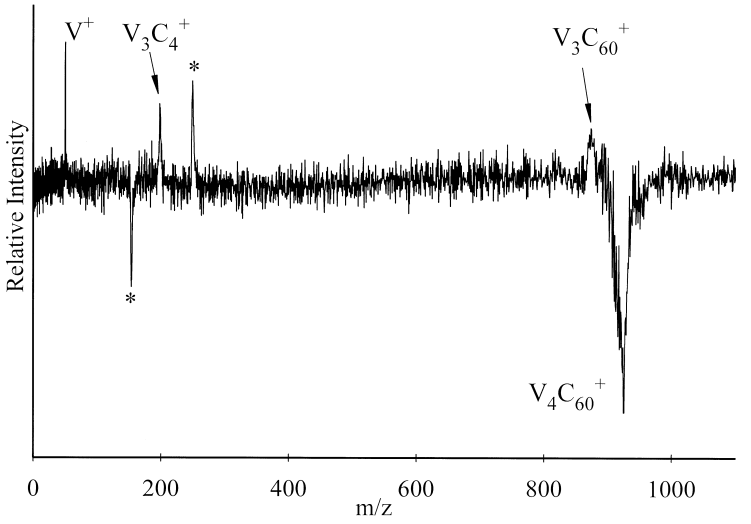

Fig. 5. Photodissociation at 355 nm of the V_4–C_{60} complex showing the efficient production of the $V_3C_4^+$ fragment. The asterisks marks known artifact peaks from electrical noise in the system.

complexes with two or three metal atoms. In these systems, there are small amounts of pure metal fragments but a large peak from C_{60}^+. The ionization potential of iron atom is greater than that of C_{60}, whereas the IPs of iron dimer and trimer are less than that of C_{60}. Thus, if molecular metal fragments are eliminated they should be charged, but if atomic metal is eliminated it should be neutral. The strong peak from C_{60}^+ therefore can be associated with the loss of neutral iron atoms from the cluster, which is then the dominant photochemical pathway. Martin and co-workers observed a strong C_{60}^+ peak when a non-mass-selected distribution of Fe_x–$(C_{60})_y$ clusters was dissociated by high intensity multiphoton ionization. They suggested that this channel of neutral iron atom loss must exist in some of these clusters. Our mass-selected measurement shows that it does indeed take place and that it is the dominant process for the clusters in this small size domain. The propensity for atom ejection suggests that these complexes have mostly separated iron atoms binding to the fullerene surface. This has also been reported recently by our lab for multi-iron complexes with the polyaromatic hydrocarbon coronene [40]. Relatively strong metal–fullerene bonding is therefore expected, so that diffusion and aggregation on the surface is inhibited. In

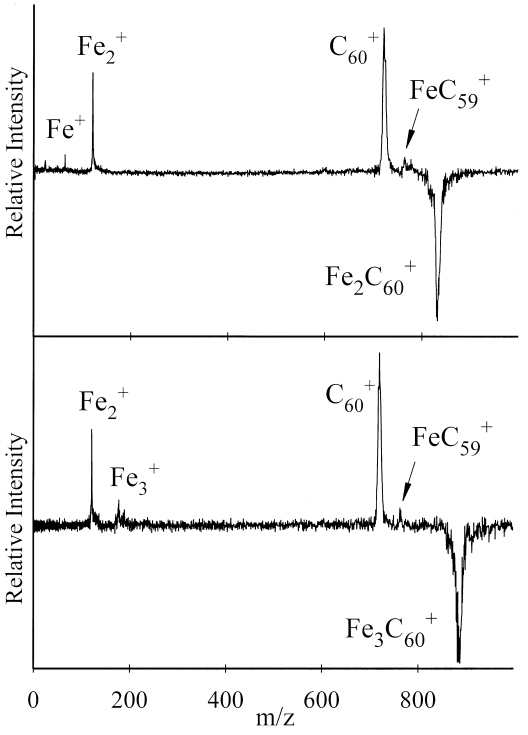

Fig. 6. Photodissociation at 355 nm of iron–C_{60} complexes with two and three metal atoms. Charged molecular iron fragments are observed as well as a strong C_{60}^+ peak. The latter peak must come from loss of neutral iron atoms. A small fragment in both spectra is $C_{59}Fe^+$.

results not shown, we observe essentially the same fragmentation channels when Co_2–C_{60}^+ and Co_3–C_{60}^+ are photodissociated.

Another fascinating observation is also consistent with strong Fe–C_{60} interactions. A weak but reproducible fragment ion is detected for both of these complexes in the mass range just above the C_{60}^+ peak. It corresponds to the fragment Fe–C_{59}^+. The formation of this mass indicates the elimination of a neutral FeC molecule (or perhaps Fe_2C from $Fe_3C_{60}^+$). The loss of separate iron and carbon atoms would be a much higher energy process. The ionization potential of FeC is not known, but this result indicates that it is greater than the IP of C_{60}. Martin and co-workers also saw this fragment when their nonselected mass distribution of $Fe_x(C_{60})_y$ was excited with multiphoton excitation [21]. They noted its formation, but did not determine which parent cluster(s) produced it. Our data shows that it is produced to some degree from even these small species, and we might speculate from the intensity of this peak seen by Martin that its yield increases for larger metal aggregates. Fe–C_{59}^+ must have either a single carbon hole in the cage, which is unlikely based on the known fragmentation of C_{60} (loss of C_2), or it must represent a metal substituted cage. Martin and co-workers have made similar observations in the fragmentation of rhodium and iridium clusters with C_{60} and C_{70}, where the masses M–C_{59} and M–C_{69} were detected [21].

Fig. 7 shows the photodissociation of $Fe(C_{60})_2^+$ and $Fe_2(C_{60})_2^+$. In both cases the only significant fragment is C_{60}^+. This shows clearly that these clusters are indeed multiple C_{60} clusters rather than M_x–C_{120} species. We have observed similar fragmentation for Fe_3–$(C_{60})_2^+$ and for $Co_{1,2}(C_{60})_2^+$. The neutral(s) lost must include either nFe + C_{60} or Fe_n–C_{60}. As before, if molecular Fe_2 or Fe_3 are eliminated, they should be charged, but these ions are not seen. Since no isolated $(C_{60})_2^+$ is seen in the mass distributions of clusters produced, and since the fragmentation indicates two C_{60} units are present, we can conclude that the metal is necessary to aggregate the fullerenes, i.e. that these masses represent sandwich structures. Sandwich formation and multidecker sandwich formation in M_x–$(C_{60})_y$ clusters has been proposed previously for other metals by Kaya and co-workers [23,25,28].

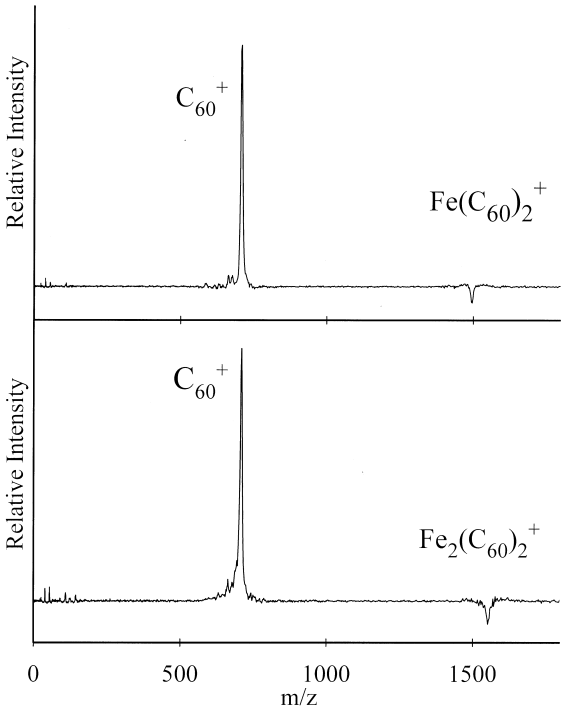

Fig. 7. Photodissociation at 355 nm of iron–$(C_{60})_2$ complexes with one and two metal atoms. The major fragment in both cases is C_{60}^+.

4. Conclusions

A variety of metal–C_{60} complexes are produced here by laser ablation/vaporization of metal rods coated with a thin film of C_{60}. This method produces mass distributions which favor the smaller cluster sizes, in contrast to the methods described by Martin and co-workers and Kaya and co-workers. The mass spectra indicate that these clusters grow by addition of metal atoms to the fullerene surface rather than by the combination of pregrown metal clusters with the fullerene. Fragmentation of these clusters is consistent with this mechanism, showing that there are both isolated atoms and aggregated atoms on the fullerene surface. Iron, vanadium, and cobalt exhibit a significant propensity toward dispersed metal atom adsorption. Several of these clusters exhibit tendencies for

metal insertion into the fullerene cage wall, as evidenced by fragmentation to form various metal carbides. In the case of vanadium, the conditions under which the clusters grow determines the degree of metal attack on the cage. The fortuitous observation of clusters produced under "cold" and warm growth conditions shows that it is the metal attack on the fullerene which causes insertion and not the photochemical reaction from the photodissociation laser. The strong tendency for carbide formation in vanadium onsets in clusters having three or more metal atoms. The previously seen cluster $Fe–C_{59}^{+}$ is shown to result in complexes containing as few as two or three metal atoms, and this cluster is suggested to represent a "metal-in-the-wall" fullerene.

The observations here and from other labs suggest that exohedral metal-fullerenes represent fascinating complexes with which to investigate metal adsorption and metal-organic insertion chemistry. It is particularly interesting to consider why the insertion processes apparently require certain critical sizes of aggregated metal and what activation energy (if any) is required. Spectroscopic studies of these systems (e.g. photoelectron spectroscopy [26]) and theoretical investigations of these issues are anticipated in the not-too-distant future.

Acknowledgements

This research is supported by the U.S. Department of Energy through contract no. DE-FG02-96ER14658.

References

[1] M.S. Dresselhaus, G. Dresselhaus, P.C. Eklund, Science of Fullerenes and Carbon Nanotubes, Academic, San Diego, 1996.
[2] A. Lahamer, Z.C. Ying, R.E. Haufler, R.L. Hettich, R.N. Compton, Adv. Met. Semicond. Clusters 4 (1998) 179.
[3] H. Shinohara, Adv. Met. Semicond. Clusters 4 (1998) 205.
[4] M. Krause, M. Hulman, H. Kuzmany, T.J.S. Dennis, M. Inakuma, H. Shinohara, J. Chem. Phys. 111 (1999) 7976.
[5] M. Takata, E. Nishibori, M. Sakata, M. Inakuma, E. Yamamoto, H. Shinohara, Phys. Rev. Lett. 83 (1999) 2214.
[6] T. Kimura, T. Sugai, H. Shinohara, Intl. J. Mass Spectrom. 188 (1999) 225.
[7] A.F. Hebard, M.J. Rosseinsky, R.C. Hadden, D.W. Murphy, S.H. Glarum, T.T.M. Palstra, A.P. Ramirez, A.P. Kortan, Nature 350 (1991) 600.
[8] G.K. Wertheim, D.N.E. Buchanan, J.E. Rowe, Science 58 (1992) 1638.
[9] P.M. Ajayan, O. Stephan, P. Redlich, C. Colliex, Nature 375 (1995) 564.
[10] P.M. Ajayan, S. Ijima, Nature 361 (1993) 333.
[11] L.M. Roth, Y. Huang, J.T. Schwedler, C.J. Cassady, D. Ben-Amotz, B. Kahr, B.S. Freiser, J. Am. Chem. Soc. 113 (1991) 6298.
[12] Y. Huang, B.S. Freiser, J. Am. Chem. Soc. 113 (1991) 8186.
[13] Y. Huang, B.S. Freiser, J. Am. Chem. Soc. 113 (1991) 9418.
[14] Q. Jiao, Y. Huang, S.A. Lee, J.R. Gord, B.S. Freiser, J. Am. Chem. Soc. 114 (1992) 2726.
[15] Y. Basir, S.L. Anderson, Chem. Phys. Lett. 243 (1995) 45.
[16] M. Welling, R.I. Thompson, H. Walther, Chem. Phys. Lett. 253 (1996) 37.
[17] T.P. Martin, N. Malinowski, U. Zimmermann, U. Naher, H.J. Schaber, J. Chem. Phys. 99 (1993) 4210.
[18] U. Zimmermann, N. Malinowski, U. Naher, S. Frank, T.P. Martin, Phys. Rev. Lett. 72 (1994) 3542.
[19] F. Tast, N. Malinowski, S. Frank, M. Heinebrodt, I.M.L. Billas, T.P. Martin, Phys. Rev. Lett. 77 (1996) 3529.
[20] F. Tast, N. Malinowski, M. Heinebrodt, I.M.L. Billas, T.P. Martin, Z. Phys. D: At., Mol., Clusters 40 (1997) 351.
[21] W. Branz, I.M.L. Billas, N. Malinowski, F. Tast, M. Heinebrodt, T.P. Martin, J. Chem. Phys. 109 (1998) 3425.
[22] J.E. Reddic, J.C. Robinson, M.A. Duncan, Chem. Phys. Lett. 279 (1997) 203.
[23] A. Nakajima, S. Nagao, H. Takeda, T. Kurikawa, K.J. Kaya, J. Chem. Phys. 107 (1997) 6491.
[24] T. Kurikawa, S. Nagao, K. Miyajima, A. Nakajima, K. Kaya, J. Phys. Chem. A 102 (1998) 1743.
[25] S. Nagao, T. Kurikawa, K. Miyajima, A. Nakajima, K. Kaya, J. Phys. Chem. A 102 (1998) 4495.
[26] B. Palpant, A. Otake, F. Hayakawa, Y. Negeshi, G.H. Lee, A. Nakajima, K. Kaya, Phys. Rev. B: Condens. Matter Mater. Phys. 60 (1999) 4509.
[27] S. Nagao, Y. Negishi, A. Kato, Y. Nakamura, A. Nakajima, K. Kaya, J. Phys. Chem. A 103 (1999) 8909.
[28] A. Nakajima, K. Kaya, J. Phys. Chem. A 104 (2000) 176.
[29] J.L. Fye, M.F. Jarrold, Int. J. Mass Spectrom. 185–187 (1999) 507.
[30] D.E. Clemmer, J.M. Hunter, K.B. Shelimov, M.F. Jarrold, Nature 372 (1994) 248.
[31] M.A. Duncan, J. Cluster Sci. 8 (1997) 239.
[32] L.R. Brock, J.S. Pilgrim, D.L. Robbins, M.A. Duncan, Rev. Sci. Instrum. 67 (1996) 2989.
[33] C.S. Yeh, J.S. Pilgrim, D.L. Robbins, K.F. Willey, M.A. Duncan, Int. Rev. Phys. Chem. 13 (1994) 231.
[34] P.B. Armentrout, D.A. Hales, L. Lian, Adv. Met. Semicond. Clusters 2 (1994) 1.
[35] J.W. Buchanan, G.A. Grieves, J.E. Reddic, M.A. Duncan, Int. J. Mass Spectrom. 182–183 (1999) 323.

[36] D.M. Cox, R.L. Whetten, M.R. Zakin, D.J. Treavor, K.C. Reichmann, A. Kaldor, Advances in Laser Science, W.C. Stwalley, M. Lapp (Eds.), AIP, New York, 1986, Vol. 1, p. 146.
[37] D.S. Yang, A.M. James, D.M. Rayner, P.A. Hackett, Chem. Phys. Lett. 231 (1994) 177.
[38] D.S. Yang, A.M. James, D.M. Rayner, P.A. Hackett, J. Chem. Phys. 102 (1995) 3129.
[39] E.A. Rohlfing, D.M. Cox, A. Kaldor, K.H. Johnson, J. Chem. Phys. 81 (1984) 3846.
[40] J.W. Buchanan, J.E. Reddic, G.A. Grieves, M.A. Duncan, J. Phys. Chem. A 102 (198) 6390.